

Thermophysical and Electrical Properties of Nanocomposites Based on Ethylene–Vinylacetate Copolymer (EVA) Filled with Expanded and Unexpanded Graphite

R. Tlili · A. Boudenne · V. Cecen ·
L. Ibos · I. Krupa · Y. Candau

Received: 21 July 2009 / Accepted: 19 June 2010 / Published online: 8 July 2010
© Springer Science+Business Media, LLC 2010

Abstract Over the last few years, conducting polymer/graphite nanocomposites have attracted considerable interest because of their exceptional electrical, thermal, and mechanical properties. Polymeric nanocomposites prepared from high aspect ratio layered graphite nanofillers achieve significant improvements in thermophysical and electrical properties at low filler concentrations, compared to conventional composites, without a significant increase in density. In this work, various aspects of the electrical and thermophysical behavior of nanocomposites are presented based on the ethylene–vinylacetate matrix filled with nanostructured expanded graphite and standard, (nano)/micro-sized graphite.

Keywords Conductive composites · Electrical conductivity · EVA · Graphite · Thermal conductivity · Thermal diffusivity

1 Introduction

Polymers are materials with very low values of thermal conductivity and electrical conductivity, which mainly depend on the degree of crystallinity [1]. However, many industrial applications including circuit boards, heat exchangers, electronics

R. Tlili · A. Boudenne (✉) · L. Ibos · Y. Candau
CERTES EA 3481 - Centre d'Etude et de Recherche en Thermique, Environnement et Systèmes,
Université Paris-Est, 61 Av. du Général de Gaulle, 94010 Créteil Cedex, France
e-mail: boudenne@u-pec.fr

V. Cecen
Mechanical Engineering Department, Dokuz Eylül University, 35100 Bornova, Izmir, Turkey

I. Krupa
Polymer Institute, Slovak Academy of Sciences, Dúbravská cesta 9, 8242 36 Bratislava, Slovakia

protection, etc. require an improvement in the thermal conductivity and (or) electrical conductivity of plastics [2,3].

One way to improve the thermal, electrical, and dielectrical behavior of these materials is to combine polymeric matrices such as thermoplastic polymers (polypropylene, polyamide, etc.), thermosetting resins (epoxy, polyurethane), or rubbers with thermally conductive fillers. Metallic or inorganic materials and graphite in several shapes (particles, fibers, nanotubes) are commonly used as thermally conductive fillers [4,5]. Very recently, some authors reported the use of carbon nanotubes as the prospective filler for the preparation of thermally conductive polymeric composites [6,7].

The association of polymer and fillers allow the creation of composites that have properties, which are intermediate between two components. Therefore, the interest for these materials arises from the fact that it is possible to develop new materials with properties adapted to specific applications. Except for graphite, metallic powders are still applied as fillers for the preparation of both highly electrically and thermally conductive composites [8]. However, metals also have some disadvantages. Most metallic fillers have a spherical shape, which induces a higher percolation threshold (*contrary to irregularly shape particles*) leading to an increase of the filler fraction in the composite, the price, and the weight of the final material.

Even though electrical and thermal properties of polymers filled with particles have been widely studied during recent years, the problem of the calculation of composite thermal and electrical properties from only a knowledge of particle sizes, concentrations, and properties of each component is still unsolved. Several theoretical or semi-empirical models have been proposed to predict thermal and electrical properties of polymeric composite materials. Nevertheless, only a few studies are devoted to a comparative analysis of both electrical and thermal properties of such two-phase systems [4–10].

In this article, we have investigated the electrical and thermophysical behavior of nanocomposites based on the ethylene–vinylacetate (EVA) matrix filled with nanostructuralized expanded graphite and standard, micro-sized graphite. The thermal and electrical conductivity of composites are compared to theoretical models.

2 Experimental

2.1 Sample Preparation

A commercial EVA copolymer, Miravithen® D 14010 V (Leuna Polymer GmbH, Germany), containing 14 mass% of vinylacetate (VA) and with a melt flow index (190 °C/2.16 kg) of 9.8 g/10 min, was chosen as the matrix. The expanded graphite GTG 5 was supplied by Graphite Technology Group, Inc. (Delaware, USA). The unexpanded graphite KS6 was supplied by Lonza Graphites and Technologies Ltd. (Sins, Switzerland).

Most particles have an aspect ratio between 20 and 250, while the expanded graphite (EG) has a size in the range from 5 μm to 6 μm in length and for unexpanded graphite (UG), from 20 μm to 25 μm.

All the composites were prepared by melt mixing in a 30 mL mixing chamber of a Brabender Plasticorder PLE 331 (Germany) at 150 °C for 10 min at a mixing speed of 35 rpm. For thermal-conductivity and thermal-diffusivity measurements, the specimens with dimensions of 50 × 50 × 4 mm³ have been compressed and molded at 120 °C for 5 min with subsequent cooling under pressure to 50 °C.

2.2 Thermal Conductivity, thermal Diffusivity, and Specific Heat Measurements

A periodical method developed by Boudenne et al. [11] was used to estimate simultaneously the thermal conductivity, thermal diffusivity, and specific heat of polymer composite materials at room temperature. This method is based on the use of a small temperature modulation in a parallelepiped-shape sample (45 mm of side length and 4 mm of thickness) and allows obtaining all of these thermophysical parameters in only one measurement with their corresponding statistical confidence bounds.

The specific heat capacities (C_p) of the composite samples were determined using thermal-conductivity and thermal-diffusivity values and knowing the density ρ :

$$C_p = \frac{k}{\rho a}. \quad (1)$$

The density measurements were achieved using square-plate samples that were used for thermal measurements. A Mettler-ToledoTM AT61 delta range balance was used to measure the mass of the samples. The sample sizes were measured using a caliper square.

2.3 Electrical Measurements

All experiments were performed using the same samples, which were used for the thermal-conductivity and thermal-diffusivity measurements (45 mm of side length and 4 mm of thickness). Two methods were used for the measurement of the volumetric electrical conductivity (Fig. 1). A four-electrode system used a Keithley 2400 source meter and Keithley 2182 nanovoltmeter for conductive composite samples ($\sigma > 10^{-5} \text{ S} \cdot \text{m}^{-1}$). A two-electrode system used a Keithley 2400 SourceMeter only for insulating samples ($\sigma < 10^{-5} \text{ S} \cdot \text{m}^{-1}$).

3 Results and Discussion

3.1 Specific Volume of Composites

The dependence of the specific density of composites on the volume filler content is shown in Fig. 2. The determination of ρ is important for checking the quality of the samples. It is clear that if composite samples are well processed, i.e., good homogeneity is reached without air bubbles in the sample as well as without unfilled pores at the polymer/filler interface, the specific density of the composites should have a linear dependence upon the volume fraction, according to the simple rule of mixtures given by

Fig. 1 Electrical-conductivity measurement setup

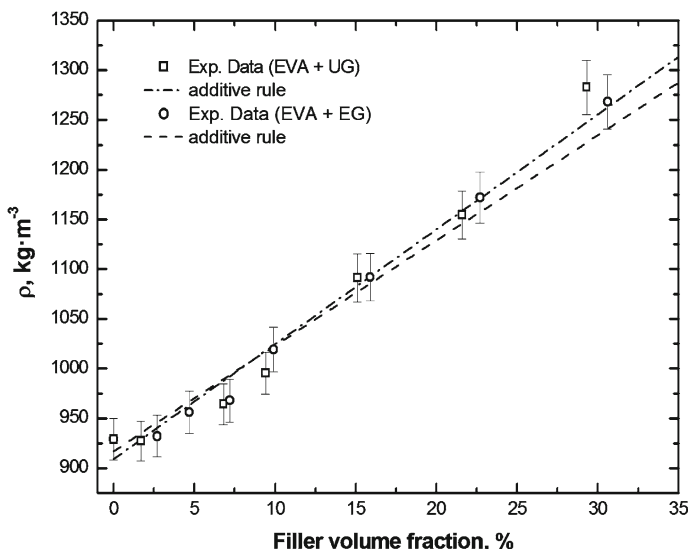
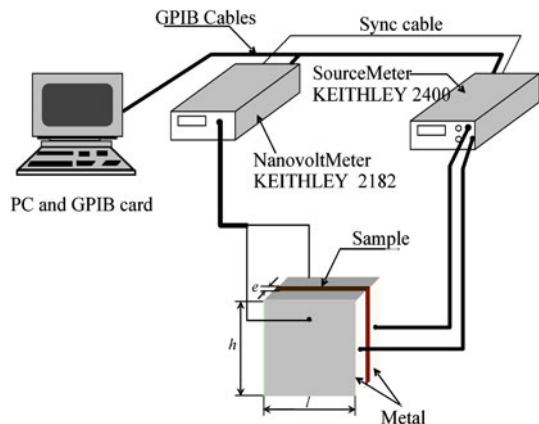


Fig. 2 Experimental data of density and mixing rule values versus filler volume fraction for EVA + UG and EVA + EG composites

$$\rho = \rho_p (1 - \varphi) + \rho_f \varphi, \quad (2)$$

where ρ_p and ρ_f are the densities of the polymeric matrix and the filler, respectively. However, the volume fraction φ is not known after processing, as the exact density of fillers mixed with the polymer is not accurately known *a priori*. Therefore, one way to obtain the value of ρ_f for each filler is to plot the specific volume V_S of the composites versus the filler mass fraction φ_m . Therefore, the variation of V_S versus φ_m should obey a linear relationship as follows:

$$V_S = V_{S,p} (1 - \varphi_m) + V_{S,f} \varphi_m = \frac{1 - \varphi_m}{\rho_p} + \frac{\varphi_m}{\rho_f} = \frac{1}{\rho} \quad (3)$$

Table 1 Specific volume and density values of polymeric matrix and fillers obtained by fitting data

Composites	$V_{S,p}$ ($\text{cm}^3 \cdot \text{g}^{-1}$)	$V_{S,f}$ ($\text{cm}^3 \cdot \text{g}^{-1}$)	ρ_p ($\text{g} \cdot \text{cm}^{-3}$)	ρ_f ($\text{g} \cdot \text{cm}^{-3}$)
EVA + UG	1.10	0.49	0.91	2.10
EVA + EG	1.09	0.51	0.92	2.00

where $V_{S,p}$ and $V_{S,f}$ are the specific volumes of the polymeric matrix and filler, respectively.

Experimental data were fitted using a linear relationship to obtain the values of $V_{S,p}$ and $V_{S,f}$. The obtained values of $V_{S,p}$ and $V_{S,f}$ and the computed values of ρ_p and ρ_f are given in Table 1.

Using the values of ρ_p and ρ_f obtained experimentally, it is possible to compute the filler volume fraction φ of each sample knowing the filler mass fraction φ_m and using the classical relationship,

$$\varphi = \frac{1}{1 + \frac{\rho_f}{\rho_p} \cdot \frac{1 - \varphi_m}{\varphi_m}}. \quad (4)$$

The values of ρ_f of composites found by fitting ($\rho_f = 2.10 \text{ g} \cdot \text{cm}^{-3}$ for composites EVA/UG and $\rho_f = 2 \text{ g} \cdot \text{cm}^{-3}$ for composites EVA/EG) are close to the literature value ($2.25 \text{ g} \cdot \text{cm}^{-3}$) [12].

It is seen from Fig. 2 that experimental data behave linearly with high accuracy according to the additive rule.

3.2 Thermal Conductivity, thermal Diffusivity, and Specific Heat

The thermal conductivity (λ) of composites and their associated uncertainties are presented in Fig. 3. An increase of λ with increasing filler content was observed for all samples investigated. This increase of λ is foreseeable because the filler has a significantly higher thermal conductivity than the polymeric matrix as will be discussed later. From Fig. 3, it is also seen that EVA/UG composites have a higher thermal conductivity than the EVA/EG ones at the same concentration. For a given concentration, the filler size and the aspect ratio affect the heat propagation in the composite.

The dependence of the thermal diffusivity transport coefficient (a) upon the filler volume fraction is shown in Fig. 4. We observe a nonlinear rise in the composite thermal diffusivity by increasing the filler concentration. This increase in thermal diffusivity is foreseeable because the fillers have a much higher thermal diffusivity than the polymer matrix. Moreover, the thermal diffusivity uncertainty is more significant at higher concentrations. We note as in the thermal conductivity case, a nonlinear increase of the composite thermal diffusivity by increasing the UG and EG filler concentration. However, the relative thermal diffusivity uncertainties are more significant at higher concentrations and higher than those noted for the thermal conductivity. Moreover, we note that the difference between the thermal diffusivity values as compared to the given concentrations for the EVA/UG and EVA/EG composites is relatively low compared to that observed for the thermal conductivity.

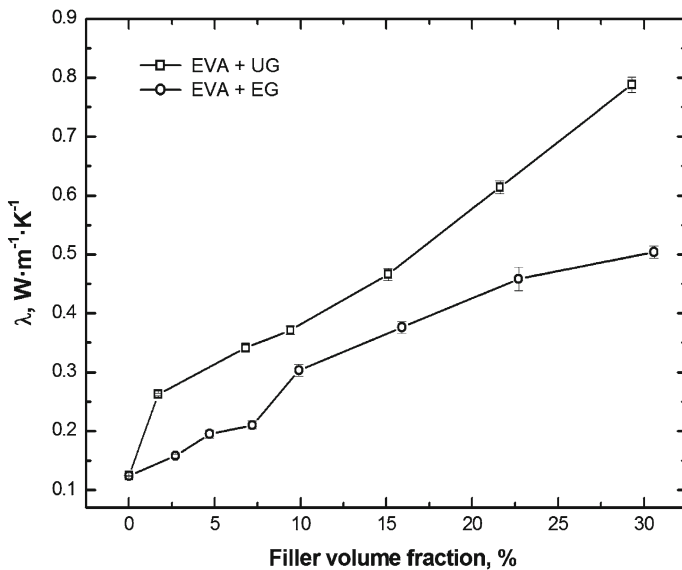


Fig. 3 Experimental values of the thermal conductivity of EVA/UG and EVA/EG composites

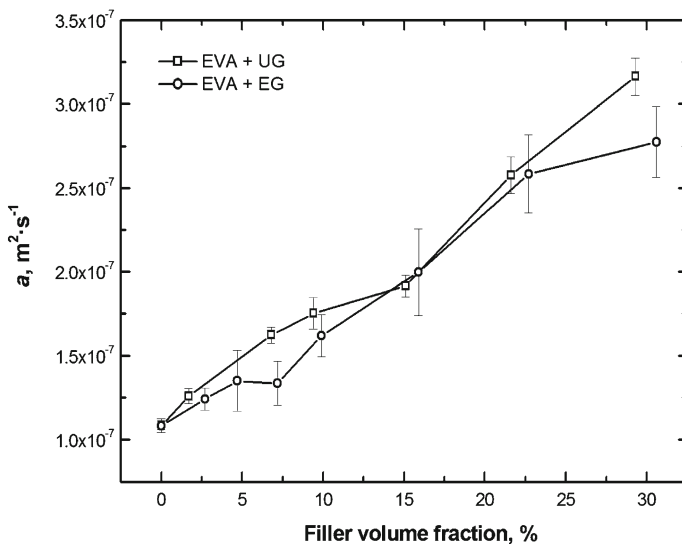


Fig. 4 Experimental values of the thermal diffusivity of EVA/UG and EVA/EG composites

The behavior of the specific heat (C_p) of EVA/UG and EVA/EG composites is depicted in Fig. 5 as a function of the filler mass fraction. We notice that for a given filler concentration, the EVA/UG composites show higher values of specific heat than do the EVA/EG ones. However, the relative uncertainties for the specific-heat values are more significant and higher than the ones noted for both the thermal conductivity and thermal diffusivity.

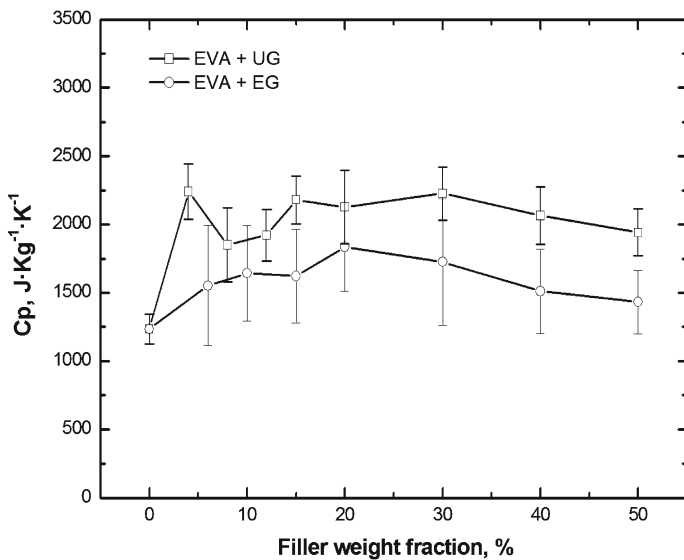


Fig. 5 Experimental values of the specific heat capacity of EVA/UG and EVA/EG composites

3.3 Thermal Conductivity Models

A deeper understanding of thermal transport in composite materials requires modeling of the thermal conductivity of heterogeneous materials by considering the influence of various parameters. Many theoretical or semi-empirical models can be found in the literature to predict the thermal conductivity of composites filled with spherical, fiber, or irregular inclusions. We have focused our study on the comparison of experimental data of the thermal conductivity of both composites with the models described below. In the following equations, λ_m is the thermal conductivity of the polymeric matrix, λ_f is the thermal conductivity of the fillers, and φ_f is the filler volume portion in the composite.

The Hatta and Taya model describes an effective thermal conductivity λ of isotropic short fiber reinforced composites according to the following equations [2, 13]:

$$\lambda = \lambda_m \left[1 + \varphi \frac{(\lambda_f - \lambda_m)(2S_{33} + S_{11}) + 3\lambda_m}{J} \right], \quad (5)$$

where

$$J = 3(1 - \varphi_f)(\lambda_f - \lambda_m)S_{11}S_{33} + \lambda_m[3(S_{11} + S_{33}) - \varphi_f(2S_{11} + S_{33})] + 3\frac{\lambda_m^2}{\lambda_f - \lambda_m} \quad (6)$$

and

$$\begin{cases} S_{11} = \frac{\frac{L}{D}}{2\left[\left(\frac{L}{D}\right)^2 - 1\right]^{3/2}} \left[\frac{L}{D} \sqrt{\left(\frac{L}{D}\right)^2 - 1} - \cosh^{-1}\left(\frac{L}{D}\right) \right] \\ S_{33} = 1 - 2S_{11} \end{cases}. \quad (7)$$

In this last equation, L is the average fiber length and D is the fiber diameter.

The Lewis and Nielsen model is defined by the following equation for various shapes of fillers [2, 14]:

$$\lambda = \lambda_m \frac{1 + AB\varphi_f}{1 - B\psi\varphi_f}, \quad (8)$$

where

$$\begin{cases} \psi = 1 + \frac{(1-\varphi_{\max})\varphi_f}{\varphi_{\max}^2} \\ B = \frac{\frac{\lambda_f}{\lambda_m} - 1}{\frac{\lambda_f}{\lambda_m} + A} \end{cases}. \quad (9)$$

A is a parameter that depends on the shape of the particles, and φ_{\max} is the maximum packing fraction. The value $\varphi_{\max} = 0.637$ is reported in the literature [2] for both graphites, randomly oriented within a polymeric matrix. However, the whole matrix must be available for filler distribution in this case. This is true for fully amorphous matrices.

In the case of a semicrystalline matrix, the crystalline part is not available for the distribution of the filler and, therefore, the above-mentioned value must be recalculated considering only the amorphous part of the polymer. We found that the degree of crystallinity of pure EVA is 28 mass%. From a knowledge of the specific density of pure EVA ($\rho_{EVA} = 0.929 \text{ g} \cdot \text{cm}^{-3}$) and from the density of the crystalline phase of polyethylene's component of EVA copolymer ($\rho_x = 0.997 \text{ g} \cdot \text{cm}^{-3}$ [15]), we can estimate the volume portion of the crystalline phase of EVA (φ_x) from

$$\varphi_x = \frac{\rho_{EVA} w_x}{\rho_x}. \quad (10)$$

Thus, the volume portion of the crystalline phase in EVA is equal to 0.26. The amorphous volume portion is 0.74, and the maximum volume fraction of the filler (φ_m^a) in EVA can be estimated as $\varphi_m^a = \varphi_x \varphi_{\max} = 0.47$. As for parameter A , according to the literature, we chose the value $A = 4.93$, which best characterize fibers with an aspect ratio equal to 10 [2].

In Fig. 6, the thermal-conductivity values obtained using Hatta and Taya and using Lewis and Nielsen are presented and are compared to measurements. All data are plotted versus the filler volume fraction. Computations were performed using the experimental value of the EVA matrix thermal conductivity ($\lambda_m = 0.124 \text{ W} \cdot \text{m}^{-1} \cdot \text{K}^{-1}$) and a value of the filler thermal conductivity ($\lambda_f = 160 \text{ W} \cdot \text{m}^{-1} \cdot \text{K}^{-1}$ for the expanded graphite (EG) and the unexpanded graphite (UG) [16]).

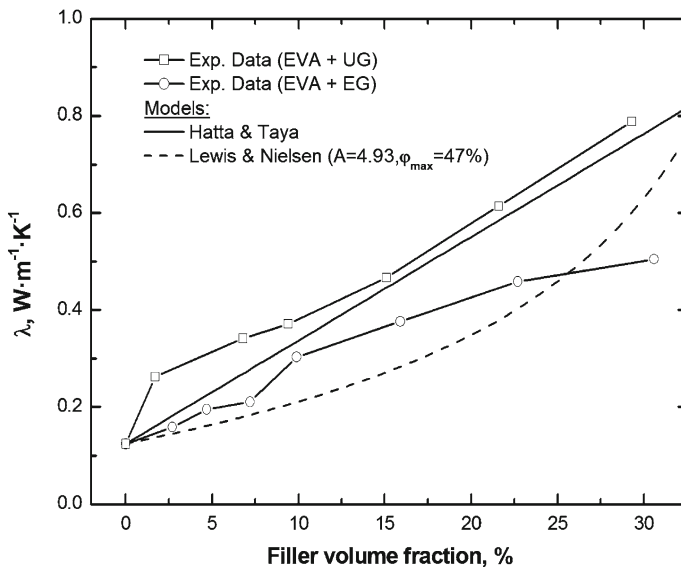


Fig. 6 Comparison between experimental values of the thermal conductivity of EVA/EG and EVA/UG composites and some theoretical models

It is seen that the Hatta and Taya model correlates well with EVA/UG composite experimental data up to 30 vol%; while the Lewis and Nielsen model underestimates the measured values. However, for the EVA/EG composite case, we notice that only the Lewis and Nielsen model, estimated the experimental thermal-conductivity values for the low filler concentrations (< 7 vol%).

Therefore, we have tried to compare the experimental data of EVA/EG composites with the Nielsen model for five coupled values of parameters A and φ_{\max} . The first two curves were computed using a theoretical value of A (equal to 4.93) and φ_{\max} (equal to 47 % and 64 % [2]), as discussed earlier (Fig. 7).

Using these values, the predictions of the Lewis and Nielsen model showed large deviations from the experimental data, except for EVA/EG composites. Then, the parameter value A was estimated by fitting experimental data and by fixing the value of the parameter φ_{\max} to 47 % and 64 %, respectively. Finally, a simultaneous estimation of both parameters was performed.

The results (values of the estimated parameters) of these fits are presented in Table 2, along with the residual norm obtained in each case. Values of the residual norm indicate that the best estimates are obtained using a φ_{\max} value close to the theoretical one considering the case of a semi-crystalline matrix, i.e., about 47 %.

The Hatta and Taya model was employed (see Fig. 8) to describe the influence of the filler thermal conductivity λ_f on the thermal conductivity of EVA/UG composites. λ_f values ranged from $2 \text{ W} \cdot \text{m}^{-1} \cdot \text{K}^{-1}$ to $200 \text{ W} \cdot \text{m}^{-1} \cdot \text{K}^{-1}$. It was found that the effect of λ_f on the thermal conductivity of composites is significant only for $\lambda_f < 50 \text{ W} \cdot \text{m}^{-1} \cdot \text{K}^{-1}$. For higher values, the effect on the model predictions becomes negligible.

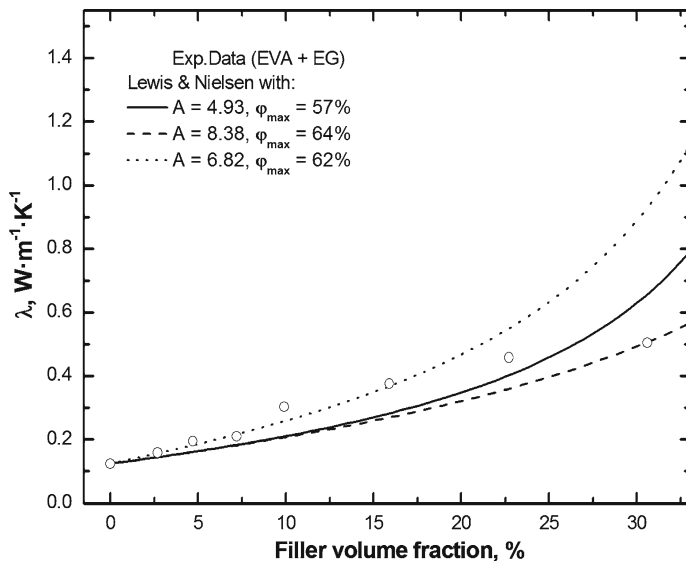


Fig. 7 Comparison of experimental values of composites EVA/EG to the Lewis and Nielsen model for different values of A and φ_{\max} parameters

Table 2 Lewis and Nielsen fitting parameters for EVA/EG composites

Parameter	A fixed and φ_{\max} free	A fixed and φ_{\max} free	A and φ_{\max} free
A	4.93	8.38	6.82
φ_{\max}	0.57	0.64	0.62

3.4 Electrical Conductivity of the Composites

For the electrical conductivity, experimental data for EVA/EG and EVA/UG composites are plotted in Fig. 9 versus the filler volume content. An increase of the electrical conductivity was observed near the percolation threshold. The percolation threshold in EVA/EG composites was found to be 6 vol%, whereas the percolation threshold in EVA/UG composites was 17 vol%.

Experimental results were compared to the statistical percolation model of Kirkpatrick and Zallen [17, 18]] (see Eq. 11) and to the model of Mamunya [19] (see Eqs. 12 and 13). The choice of these models was based on two reasons: the model of Kirkpatrick and Zallen is the basis for many recent thermal conductivity models; and the model of Mamunya, among the models developed recently, provides good agreement between the calculated values and the experimental data.

Kirkpatrick:

$$\sigma = \sigma_0 (\varphi - \varphi_c)^t \quad (11)$$

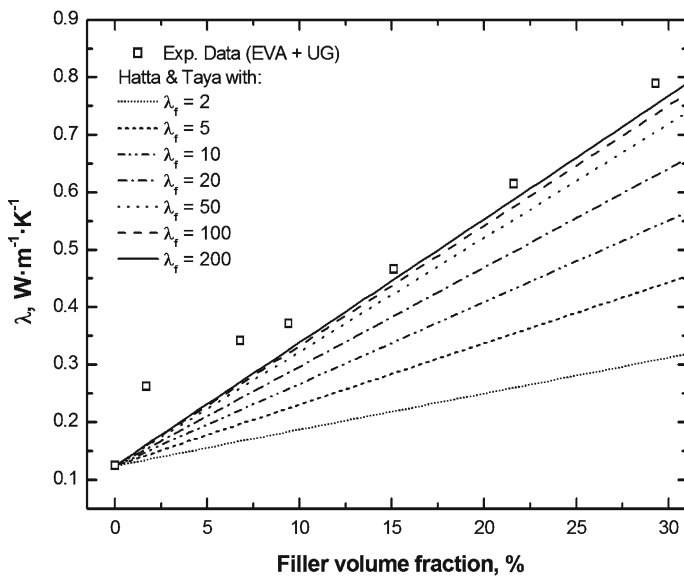


Fig. 8 Variation of the thermal conductivity of composites according to the Hatta and Taya model using different values of the thermal conductivity of fillers λ_f

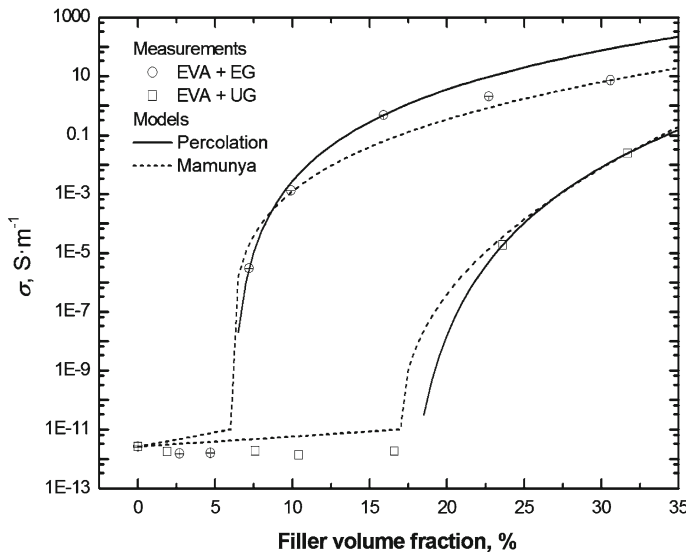


Fig. 9 Electrical conductivity (measured at 25 °C) of composites as a function of filler volume content: experimental data and fitted models

Mamunya:

$$\log \sigma = \log \sigma_p + (\log \sigma_c - \log \sigma_p) \frac{\varphi}{\varphi_c} \quad (12)$$

Table 3 Values of estimated fitting parameters

Composite	Percolation model		Mamunya model	
	σ_0 ($\text{S} \cdot \text{m}^{-1}$)	t	σ_m ($\text{S} \cdot \text{m}^{-1}$)	k
EVA + EG	2.52×10^5	5.68	7.2	0.21
EVA + UG	7.23×10^5	8.96	0.0246	0.45

when $\varphi < \varphi_c$

$$\log \sigma = \log \sigma_c + (\log \sigma_m - \log \sigma_c) \left(\frac{\varphi - \varphi_c}{F - \varphi_c} \right)^k \quad (13)$$

when $\varphi > \varphi_c$.

In Eqs. 11–13, t is a critical exponent, φ is the filler volume fraction, φ_c is the volume content at the percolation threshold (determined experimentally in all cases), σ is the composite electrical conductivity, σ_0 is the electrical conductivity of the fillers, σ_c is the electrical conductivity at the percolation threshold, σ_m is the electrical conductivity at the maximum packing fraction F , σ_p is the electrical conductivity of the polymeric matrix, and the exponent k depends on the interactions between the polymer matrix and filler [19]. The value of k is not the same for various composites [4, 19].

The curves calculated according to the model of Mamunya and to the percolation model were plotted in Fig. 9. According to this figure, both models provide a correct estimation of the electrical conductivity of composites. This is expected because both models are semi-empirical and the fitting parameters are given in Table 3.

As for the percolation coefficient t , it is seen that its value is higher than those computed from percolation theory. Kirkpatrick [18] gave the following values for the critical exponent t :

$$t = 1.6 \pm 0.1 \text{ (for the bond percolation model),}$$

$$t = 1.5 \pm 0.1 \text{ (for the point percolation model).}$$

However, other critical exponents can also be found in the literature. According to Tchmutin et al. [20], the critical exponent for a three-dimensional system is $t = 1.6$ to 1.9, while the percolation concentration is 0.17. The discrepancy between theoretical values and the fitted result is due to the fact that the Kirkpatrick model does not take into account the peculiarities of the specific system structure, mainly the particle shape, polymer–filler interaction, existence of contact phenomena on the particle–particle boundary, and the influence of preparation conditions on the volume distribution of conductive particles. In our case, the graphitic sheets are too far from a spherical shape, which results in both lower percolation thresholds which belongs to the spheres dispersed within a matrix and in a higher electrical conductivity, which is represented by a more pronounced percolation coefficient.

4 Conclusion

The thermal and electrical behavior of EVA filled with nanostructuralized expanded graphite and standard, (nano)/micro-sized graphite were investigated. The thermal conductivity and thermal diffusivity of each composite were studied for various filler volume concentrations. The thermophysical properties of these nanocomposites are higher than for the neat matrix. However, the filler size and the aspect ratio affect the heat propagation in the composite and the thermophysical behavior. Besides, we have shown that the structure of the graphite affects also the electrical behavior and the electrical percolation threshold, which in EVA/EG composites was found to be 6 vol% and 17 vol% in EVA/UG composites.

Acknowledgments The research was supported by the Scientific Grant Agency of the Ministry of Education of the Slovak Republic and the Slovak Academy of Sciences (Project no. 2/0063/09) and by Science and Technology Assistance Agency under contract no. APVV-0478-07. The Scientific and Technological Research Council of Turkey TUBITAK is acknowledged for the granting of V. Cecen postdoctoral study in the framework of the TUBITAK-BIDEB 2219-International Postdoctoral Research Scholarship Program.

References

1. J. Banrup, E. Immergut, E. Grulke, *Polymer Handbook*, 4th edn. (John Wiley & Sons Inc., New York, 1999)
2. D.M. Bigg, *Adv. Polym. Sci.* **119**, 1 (1995)
3. Z.M. Huang, Y.Z. Zhang, M. Kotaki, S. Ramakrishna, *Compos. Sci. Technol.* **63**, 2223 (2003)
4. Y.P. Mamunya, V.V. Davydenko, P. Pissis, E.V. Lebedev, *Eur. Polym. J.* **38**, 1887 (2002)
5. I. Krupa, A. Boudenne, L. Ibos, *Eur. Polym. J.* **43**, 2443 (2007)
6. Q.Z. Xue, *Physica B* **368**, 302 (2005)
7. Y.P. Mamunya, A. Boudenne, N. Lebovka, L. Ibos, Y. Candau, M. Lisunova, *Compos. Sci. Technol.* **68**, 1981 (2008)
8. A. Boudenne, L. Ibos, E. Géhin, M. Fois, J.C. Majesté, *J. Mater. Sci.* **40**, 4163 (2005)
9. Z. Wen, T. Itoh, T. Uno, M. Kubo, O. Yamamoto, *Solid State Ion.* **160**, 141 (2003)
10. D.W. Sundstrom, Y.D. Lee, *J. Appl. Polym. Sci.* **16**, 3159 (1972)
11. A. Boudenne, L. Ibos, Y. Candau, *Meas. Sci. Technol.* **17**, 1870 (2006)
12. G. Wypych, *Handbook of Fillers* (ChemTec Publishing, Toronto, Canada, 1999)
13. H. Hatta, M. Taya, *J. Appl. Phys.* **59**, 1851 (1986)
14. T.B. Lewis, L.E. Nielsen, *J. Appl. Polym. Sci.* **14**, 1449 (1970)
15. K. Eiermann, *Kolloid-Z.* **201**, 3 (1965)
16. R.L. Powell, G.E. Childs, in *American Institute of Physics Handbook* (McGraw-Hill, New York, 1972), pp. 4-142–4-160
17. F. Lux, *J. Mater. Sci.* **28**, 285 (1993)
18. S. Kirkpatrick, *Rev. Mod. Phys.* **45**, 574 (1973)
19. E.P. Mamunya, V.V. Davydenko, E.V. Lebedev, *Compos. Interfaces* **4**, 169 (1997)
20. I.A. Tchmutin, A.T. Ponomarenko, V.G. Schevchenko, D.Y. Godovski, *Synth. Met.* **66**, 19 (1994)